

Analysis of the Transfer-Function Models of Electric Drives with Controlled Voltage Source

Abstract. The mathematical models of the DC and AC motors are introduced and compared. The voltage control of motor without decoupling is considered. The flux linkage generation (rotor or stator) and electromagnetic torque are analysed. Models were unified to the transfer-function form. Mathematically proved that the transfer-function: flux linkage to the voltage in the flux axis d is always the lag element. However, the transfer-function: electromagnetic torque to voltage in the torque axis q can be the oscillatory or lag element with the difference. The propositions of the flux and torque control systems are introduced.

Streszczenie. Przedstawiono i porównano modele matematyczne silników prądu stałego i przemiennego. Rozważono sterowanie napięciowe silnikami bez odsprzęgania. Analizie poddano wytwarzanie strumienia skojarzonego (wirnika lub stojana) oraz momentu elektromagnetycznego. Modele zostały ujednoczone do postaci transmitancji. Udowodniono, że transmitancja: strumień skojarzony do napięcia w osi strumienia d jest zawsze obiektem inercyjnym. Natomiast transmitancja: moment elektromagnetyczny do napięcia w osi momentu q może być obiektem oscylacyjnym lub inercyjnym z różniczką. Przedstawiono propozycje układów regulacji strumienia i momentu. (Analiza transmitancyjnych modeli napędów elektrycznych ze sterowanym źródłem napięciowym)

Keywords: transfer-function, controlled voltage source, separately excited DC motor, permanent magnet synchronous motor (PMSM), brushless DC (BLDC) motor, induction motor, vector control.

Słowa kluczowe: transmitancja, sterowane źródło napięcia, silnik obcoważony prądu stałego, silnik synchroniczny z magnesami trwałymi (PMSM), bezszczotkowy silnik prądu stałego (BLDC), silnik indukcyjny, sterowanie wektorowe.

Introduction

In modern drives the controlled voltage sources are most often applied as the power supply of the electric motor (thyristor-controlled converter or voltage-source inverter) [1, 2, 3, 4, 5, 6, 7].

In the aim of the synthesis of the electrical drives control system designers use the mathematical models in the transfer-function form most frequently. The errors of the parameters identification, nonlinearities and the temperature influence (resistances of the windings) [3] are usually omitted in these models (motor and power converter). Thus, the additional tests of the control system robustness should be realized.

In the case of AC motor signals decoupling is used, which from one side introduces additional disadvantageous feedbacks, and on the other side simplifies models to the first order lag elements. [2, 4, 7, 8].

In the paper the mathematical models of the drives without decoupling systems are considered.

The fundamental system of electromagnetic equations for any electric motor is [1, 9]

$$(1a) \quad \underline{u}_S = R_S \dot{\underline{i}}_S + \frac{d\underline{\psi}_S}{dt} + j\omega^K \underline{\psi}_S$$

$$(1b) \quad \underline{u}_R = R_R \dot{\underline{i}}_R + \frac{d\underline{\psi}_R}{dt} + j(\omega^K - p_b \omega_m) \underline{\psi}_R$$

$$(1c) \quad \underline{\psi}_S = L_S \dot{\underline{i}}_S + L_{\mu} \dot{\underline{i}}_R$$

$$(1d) \quad \underline{\psi}_R = L_R \dot{\underline{i}}_R + L_{\mu} \dot{\underline{i}}_S.$$

where ω^K is the angular speed of rotating coordinate system (reference frame).

Depending on motor construction (AC or DC), the method of the supply and the coordinate system (stationary or rotating with the rotor or stator flux) the above mentioned model becomes transformed to the desirable form.

The complement of above mentioned equations is mechanical equation (for $J = const.$ – total inertia of motor and load reduced to motor shaft) [1, 2, 5, 8, 10]

$$(2) \quad J \frac{d\omega_m(t)}{dt} = M_e(t) - M_m(t)$$

where M_m is load torque and M_e is electromagnetic torque,

which depends on the reference frame [7].

In the parametric optimization of the controllers the model of the power converter is represented as [1, 2, 3, 5]:

$$(3) \quad G_p(s) = K_p e^{-\tau_0 s} \approx \frac{K_p}{\tau_0 s + 1}$$

Separately Excited DC motor

Current in the excitation circuit has constant value I_m , which generates flux rotary linked with armature winding with a rated value ψ_e . The electric drive (fig. 1) consists of the controller, power amplifier being a thyristor converter, supplying the separately excited DC motor.

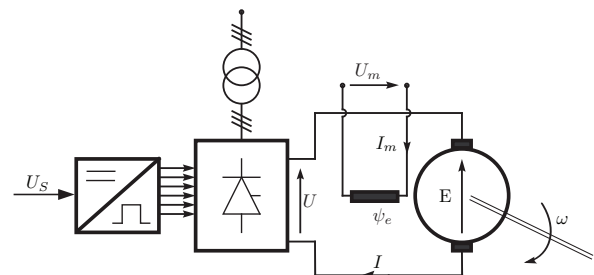


Fig. 1. Voltage control of the separately excited DC motor

From equations (1) and (2) mathematical model of the separately excited DC motor according to [1, 11, 9] is described by the following differential equations ($U_m = u_{Sd}, U = u_{Sq}$)

$$(4a) \quad U_m = R_m I_m + L_m \frac{dI_m}{dt}$$

$$(4b) \quad U = R_R I + L_R \frac{dI}{dt} + \underbrace{k_{\psi} L_{\mu} f(I_m) \omega}_{\approx \psi_e}, \quad E = \psi_e \omega$$

$$(4c) \quad J \frac{d\omega}{dt} = M_e - M_m, \quad M_e = \psi_e I$$

where f is nonlinear magnetizing curve.

The mathematical model may be presented in the functional diagram form as in fig. 2, where $G_p(s)$ is the transfer-function of thyristor static converter.

Thus, the input-output transfer-functions are in the following form ($U = u_{Sq}, U_m = u_{Sd}, I = i_{Sq}, \psi_e = \psi_{Sd}$):

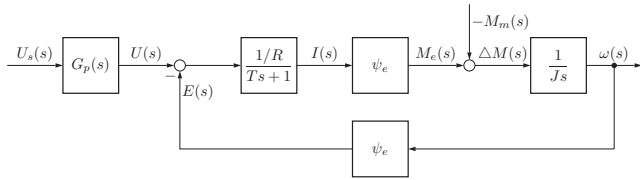


Fig. 2. Functional diagram of the separately excited DC motor

$$(5a) \quad G_{\omega U}(s) \Big|_{M_m=0} = \frac{\omega(s)}{U(s)} = \frac{\frac{1}{e}}{BTs^2 + Bs + 1}$$

$$(5b) \quad G_{\omega M}(s) \Big|_{U=0} = \frac{\omega(s)}{M_m(s)} = \frac{\frac{R}{e}(Ts + 1)}{BTs^2 + Bs + 1}$$

$$(5c) \quad G_{IU}(s) \Big|_{M_m=0} = \frac{I(s)}{U(s)} = \frac{\frac{B}{R}s}{BTs^2 + Bs + 1}$$

$$(5d) \quad G_{IM}(s) \Big|_{U=0} = \frac{I(s)}{M_m(s)} = \frac{\frac{1}{e}}{BTs^2 + Bs + 1}$$

$$(5e) \quad G_{\psi}(s) = \frac{\psi_e(s)}{U_m(s)} = \frac{\frac{k_{\psi}}{R_m}}{T_m s + 1}$$

where

$$(5f) \quad B = J \frac{R}{e}, \quad T = \frac{L}{R}, \quad T_m = \frac{L_m}{R_m}$$

are the electromechanical and electromagnetic time constants.

Taking into consideration expression $M_e = \psi_e I$, **the control of the torque with the constant flux ψ_e leads to the control of the armature current I .**

The motor torque from the functional diagram (fig. 2) equals

$$(6) \quad M_e = \underbrace{\frac{\frac{B}{R\psi_e}s}{BTs^2 + Bs + 1}}_{G_M(s)} U + \underbrace{\frac{1}{BTs^2 + Bs + 1}}_{G_{d1}(s)} M_m$$

BLDC Motor

The BLDC motors require the uses of power electronic inverters (the most often the Voltage Source Inverter) to aim the proper realization of the commutation process. This means, that inverter realizes the function of the commutator (electronic commutator) with the simultaneous control of the average value of the voltage (PWM method).

The model derives for the observed motor before the electronic commutator. Due to the principle of the motor power supply, that is flow of current in every moment of control by 2 stator winding, we take the equivalent of resistance and the inductance of the armature of the separately excited DC motor [3]

$$(7) \quad R = 2R_S, \quad L = 2(L_S - M), \quad T = \frac{L}{R}$$

where R_S , L_S are resistance and inductance of one stator winding and M is mutual inductance between stator inductances.

The flux produced by the motor rotor (the equivalent of the flux linkage of armature winding for the separately excited motor) is determined by the torque constant k_t or SEM constant k_E :

$$(8) \quad \psi_e \approx k_t \sqrt{\frac{2}{3}} \approx k_E \sqrt{\frac{2}{3}}$$

The current I means the peak value ($I_N = \sqrt{\frac{3}{2}} I_{NRMS}$, where I_{NRMS} is passed on rated plate or catalogue card).

Squirrel-Cage Induction Motor - RFOC Method

The position of the rotor flux linkage is the reference frame in RFOC (Rotor Field Oriented Control) [1, 2, 3, 4, 5, 7, 8, 12, 13]:

$$(9) \quad \begin{aligned} \underline{\psi}_R &= L_R \dot{i}_R + L_{\mu} \dot{i}_S = L_{\mu} \dot{i}_{mR}, \\ \dot{i}_{mR} &= \frac{\psi_R}{L_{\mu}} = \frac{L_R}{L_{\mu}} \dot{i}_R + \dot{i}_S \end{aligned}$$

so

$$(10) \quad \underline{\psi}_R = |\underline{\psi}_R| = \psi_R = L_{\mu} |\dot{i}_{mR}| = L_{\mu} i_{mR}$$

the reference frame rotates with the speed

$$(11) \quad \omega_{mR} = \frac{d\varrho_R}{dt} = p_b \omega_m + \frac{i_{Sq}}{T_R i_{mR}} = p_b \omega_m + \omega_2$$

Currents with reference axes oriented to the rotor flux are presented in fig. 3.

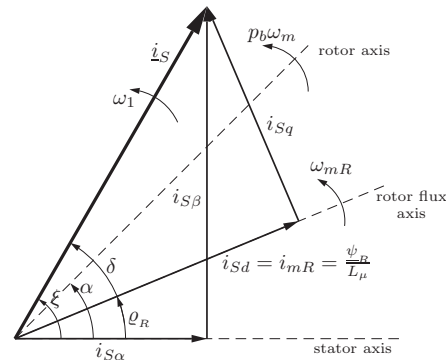


Fig. 3. Steady-state vector diagram for RFOC method

On the basis of the equations (1),(10) and (11) is obtained [5]

$$(12a) \quad \begin{aligned} u_{sd} &= R_S i_{sd} + (1 - \sigma) L_S \frac{di_{mR}}{dt} \\ &+ \sigma L_S \left(\frac{di_{sd}}{dt} - i_{sq} \omega_{mR} \right) \end{aligned}$$

$$(12b) \quad \begin{aligned} u_{sq} &= R_S i_{sq} + (1 - \sigma) L_S i_{mR} \omega_{mR} \\ &+ \sigma L_S \left(\frac{di_{sq}}{dt} + i_{sd} \omega_{mR} \right) \end{aligned}$$

$$(12c) \quad T_R \frac{di_{mR}}{dt} + i_{mR} = i_{sd}$$

and (2) is in the form

$$(13) \quad J \frac{d\omega_m}{dt} = \underbrace{\frac{3}{2} p_b (1 - \sigma) L_S i_{mR} i_{sq}}_K - M_m$$

The equation (12c) and its derivative is substituted to the equation (12a), which leads to

$$(14) \quad \begin{aligned} u_{sd} &= \sigma L_S T_R \frac{d^2 i_{mR}}{dt^2} + (R_S T_R + L_S) \frac{di_{mR}}{dt} \\ &+ R_S i_{mR} - \sigma L_S i_{sq} \omega_{mR} \end{aligned}$$

or in the Laplace transform

$$(15) \quad i_{mR}(s) = \frac{1/R_S u_{Sd} + \sigma T_S \overbrace{\mathcal{L}\{\omega_{mR} i_{Sq}\}}^{d_{im}}}{\sigma T_R T_S s^2 + (T_R + T_S)s + 1}$$

where \mathcal{L} is the transform.

The characteristic polynomial of the transfer-function (15) has always real eigenvalues (2nd order lag element):

$$(16) \quad \Delta = T_R^2 + T_S^2 + 2T_R T_S - 4\sigma T_R T_S > 0$$

This results from the fact, that typically $0.05 < \sigma < 0.2$.

This indicates that (15) can be written in the form:

$$(17a) \quad i_{mR}(s) = \frac{1/R_S u_{Sd} + \sigma T_S d_{im}}{(T_1 s + 1)(T_2 s + 1)}$$

where time constants are

$$(17b) \quad T_1 = \frac{2\sigma T_R T_S}{T_R + T_S - \sqrt{\Delta}}, \quad T_2 = \frac{2\sigma T_R T_S}{T_R + T_S + \sqrt{\Delta}}$$

From (17b) it results that $T_1 > T_2$.

The signal d_{im} from equations (15) and (17a) is recognised as disturbance on which control system has to be robusted.

On the basis of (10) and (17a) transfer-function can be determined

$$(17c) \quad \psi_R(s) = \underbrace{\frac{\frac{L_\mu}{R_S}}{(T_1 s + 1)(T_2 s + 1)}}_{G_\psi} u_{Sd} + \underbrace{\frac{\sigma L_\mu T_S}{(T_1 s + 1)(T_2 s + 1)}}_{G_{di}} d_{im}$$

Assuming that $i_{mR} = const.$ the equation (12b) can be written in the Laplace transforms form

$$(18) \quad i_{Sq}(s) = \frac{1/R_S (u_{Sq} - L_S \mathcal{L}\{i_{mR} \omega_{mR}\})}{\sigma T_S s + 1}$$

After completing the equation (18) by (11) and (13) the mathematical model is obtained in the functional diagram (fig. 4), which can be transformed to the structure in fig. 5 and finally to the diagram introduced in fig. 6.

The transformation of the block diagram does not require to using any decoupling system.

COROLLARY: At constant value of the current i_{mR} or flux ψ_R the control system of the electromagnetic torque (M_e) is linear.

The motor transfer-function in fig. 6 can be described by the following relationship:

$$(19a) \quad G_{iq} = \frac{i_{sq}(s)}{u_{sq}(s)} = \frac{\frac{1}{\sigma L_S} B T_S}{B T_S^2 + B s + 1}$$

where the coefficients are

$$(19b) \quad B = \frac{J(T_R + T_S)}{T_R T_S i_{mR}^2 p_b K}, \quad T = \frac{\sigma T_R T_S}{T_R + T_S}$$

Transfer-function (19) is in the form of (5c) and for RFOC system the relationship (6) is true .

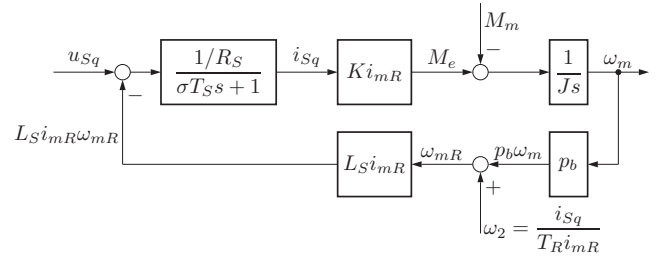


Fig. 4. Control of i_{Sq} – basic model

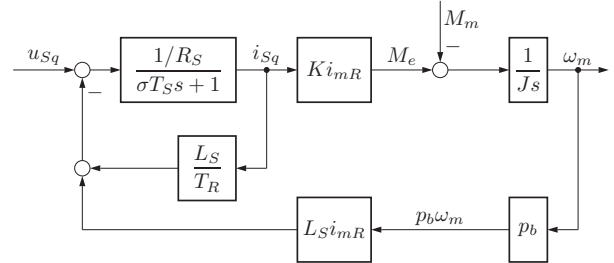


Fig. 5. Control of i_{Sq} – transformed model

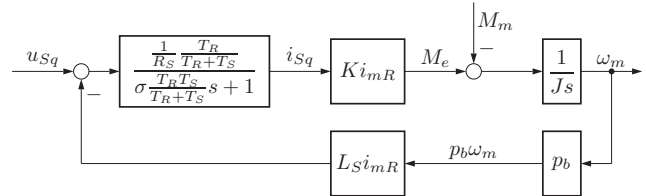


Fig. 6. Control of i_{Sq} – equivalent block diagram

Squirrel-Cage Induction Motor - SFOC and DTC-SVM Methods

The review of the most often applied methods was presented in the work [14].

The method DTC-SVM (Direct Torque Control-Space Vector Modulation) was proposed in [15] and developed e.g. in the works [2, 8, 16, 17, 18], where the aim of the mathematical model simplification a decoupling system is applied. Another approach [19, 20, 21] is the approximation of induction motor model to the transfer-function form.

SFOC (Stator Field Oriented Control) and DTC-SVM methods are realized for stator flux reference frame ($\omega^K = \omega_{mS}$):

$$(20) \quad \underline{\psi}_S = \psi_{Sd} + \underbrace{j\psi_{Sq}}_{=0} = |\underline{\psi}_S| = \psi_S$$

and the mechanical equation is described in the following form

$$(21) \quad J \frac{d\omega_m}{dt} = \underbrace{\frac{3}{2} p_b \psi_S i_{Sq}}_{M_e} - M_m$$

Currents, voltage and fluxes with reference axes oriented to the stator flux are presented in fig. 7.

Substitution (20) to (1) leads to [19, 20, 21]:

$$(22) \quad R_R L_S u_{Sd} + \sigma L_S L_R \frac{d u_{Sd}}{dt} = R_R R_S \psi_S + \underbrace{\sigma L_S L_R}_{L_S L_R - L_\mu^2} \frac{d^2 \psi_S}{dt^2} + (R_R L_S + R_S L_R) \frac{d \psi_S}{dt} + (\omega_{mS} - p_b \omega_m) \sigma L_S L_R i_{Sq}$$

and after applying the Laplace transform transfer-function of

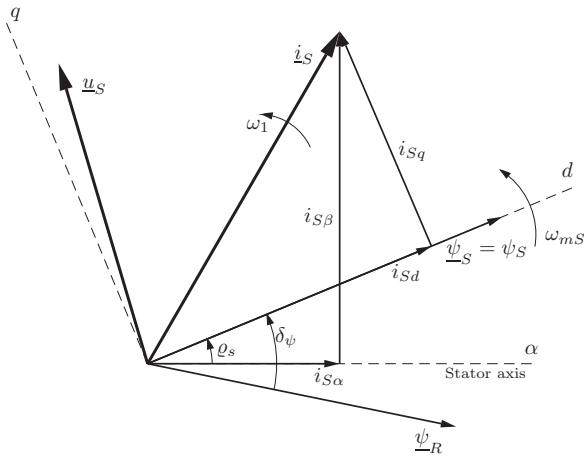


Fig. 7. Steady-state vector diagram for SFOC and DTC-SVM methods

the stator flux circuit is obtained in the following equation (23a)

$$\psi_S = \frac{T_S(\sigma T_R s + 1)u_{sd} - \sigma T_S T_R \mathcal{L}\{(\omega_{mS} - p_b \omega_m)i_{sq}\}}{\sigma T_R T_S s^2 + (T_R + T_S)s + 1} \quad (23a)$$

Relationship (23a) has characteristic polynomial identical as (15), and can be described in similar form.

$$\psi_S(s) = \underbrace{\frac{T_S(\sigma T_R s + 1)}{(T_1 s + 1)(T_2 s + 1)}}_{G_\psi} u_{sd} - \underbrace{\frac{\sigma T_S T_R}{(T_1 s + 1)(T_2 s + 1)}}_{G_{di}} d_{im} \quad (23b)$$

To determine relationship which describes electromagnetic torque the equation (1) is transformed to the following form [19, 20, 21]:

$$(R_R L_S + R_S L_R)i_{sq} + \sigma L_S L_R \frac{di_{sq}}{dt} = L_R u_{sq} - p_b \omega_m \psi_S L_R + (p_b \omega_m - \omega_{mS})\sigma L_S L_R i_{sd} \quad (24)$$

where authors assumed that

$$(p_b \omega_m - \omega_{mS})\sigma L_S L_R i_{sd} \approx 0, \quad M_m = 0 \quad (25)$$

and obtained transfer-function, which gives very good results for motor starting and braking without load torque. In the aim of the classical robust control [22, 23, 24] the influence of M_m and $(p_b \omega_m - \omega_{mS})i_{sd}$ should be assigned in motor torque. Thus, the equation (24) after substituting (21) and applying the Laplace transform is described by the following relationship

$$(R_R L_S + R_S L_R)i_{sq} + \sigma L_S L_R i_{sq} s = L_R u_{sq} - \frac{3 p_b^2 L_R \psi_S^2}{2 J} \frac{1}{s} i_{sq} + \frac{p_b L_R \psi_S}{J} \frac{1}{s} M_m + \sigma L_S L_R \mathcal{L}\{(p_b \omega_m - \omega_{mS})i_{sd}\} \quad (26)$$

After multiplication of the equation (26) by s and $\frac{2}{3} \frac{J}{p_b^2 L_R \psi_S^2}$ transfer-function form is obtained

$$i_{sq} = \underbrace{\frac{\frac{2}{3} \frac{J}{p_b^2 \psi_S^2} s}{B T s^2 + B s + 1}}_{G_{iq}(s)} u_{sq} + \underbrace{\frac{\frac{2}{3} \frac{1}{p_b \psi_S}}{B T s^2 + B s + 1}}_{G_{d1}(s)} M_m + \underbrace{\frac{\frac{2}{3} \frac{\sigma L_S J}{p_b^2 \psi_S^2} s}{B T s^2 + B s + 1}}_{G_{d2}(s)} \mathcal{L}\{(p_b \omega_m - \omega_{mS})i_{sd}\} \quad (27a)$$

where

$$B = \frac{2 J (T_R + T_S) R_s}{3 p_b^2 \psi_S^2 T_R}, \quad T = \frac{\sigma T_R T_S}{T_R + T_S} \quad (27b)$$

The transfer-function (27) refers to SFOC method [1, 5, 10]. And for DTC-SVM, according to (21): $i_{sq} = \frac{2}{3} \frac{1}{p_b \psi_S} M_m$, the relationship in the following form is obtained

$$M_e = \underbrace{\frac{\frac{J}{p_b \psi_S} s}{B T s^2 + B s + 1}}_{G_{Mq}(s)} u_{sq} + \underbrace{\frac{1}{B T s^2 + B s + 1}}_{G_{d1}(s)} M_m + \underbrace{\frac{\frac{\sigma L_S J}{p_b \psi_S} s}{B T s^2 + B s + 1}}_{G_{d2}(s)} \underbrace{\mathcal{L}\{(p_b \omega_m - \omega_{mS})i_{sd}\}}_{d_{\omega_i}} \quad (28)$$

The transfer-function (28) is the extension of (6) and signal d_{ω_i} indicates that motor torque model is nonlinear.

PMSM

Rotor reference frame $\omega^K = p_b \omega_m$ is predominantly used for PMSM control and from equations (1) the following equations are obtained [1, 2, 5, 12, 25, 26]:

$$u_{sd} = R_S i_{sd} + \frac{d\psi_{sd}}{dt} - p_b \omega_m \psi_{sq} \quad (29a)$$

$$u_{sq} = R_S i_{sq} + \frac{d\psi_{sq}}{dt} + p_b \omega_m \psi_{sd} \quad (29b)$$

$$\psi_{sd} = L_d i_{sd} + \psi_f \quad (29c)$$

$$\psi_{sq} = L_q i_{sq} \quad (29d)$$

$$M_e = \frac{3}{2} p_b (\psi_{sd} i_{sq} - \psi_{sq} i_{sd}) \quad (29e)$$

where L_d i L_q are direct and quadrature axis stator self-inductances in rotor reference frames.

The vector position $\underline{\psi}_f$ is identical to rotor d axis and hence $|\underline{\psi}_f| = \psi_f$.

Usually $i_{sd} = 0$ (system without field-weakening) , i.e. $\psi_{sd} = \psi_f$, and equations (29) are described in the following form:

$$u_{sq} = R_S i_{sq} + \frac{d\psi_{sq}}{dt} + p_b \omega_m \psi_f \quad (30)$$

$$\psi_{sq} = L_q i_{sq} \quad (31)$$

$$J \frac{d\omega_m}{dt} = \frac{3}{2} p_b \psi_f i_{sq} - M_m, \quad (32)$$

After substitution (31) to (30) stator equation is obtained

$$u_{sq} = R_S i_{sq} + L_q \frac{di_{sq}}{dt} + p_b \omega_m \psi_f, \quad \omega = p_b \omega_m \quad (33)$$

From (33) it results that induced emf equals

$$E = \omega \psi_f = p_b \omega_m \psi_f \quad (34)$$

On the basis of equations (32),(33),(34) block diagram of PMSM can be realized as in fig. 8, where $T_S = \frac{L_q}{R_S}$ is the electromagnetic time constant of stator in q axis.

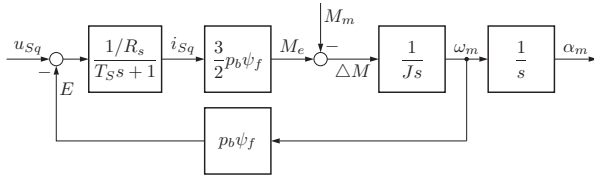


Fig. 8. Equivalent block diagram of PMSM ($i_{Sd} = 0$)

From fig. 8 it can be noticed that electromagnetic torque is in the form (6).

Mathematical models analysis

Flux circuit

Transfer-functions (5e), (17) and (23b) are similar and they are always lag elements, which are subjected to disturbance d_{im} . Dynamics (transfer-function denominator) of the induction motor flux control circuit do not depend on reference frame (RFOC or SFOC).

The control system of the flux linkage ψ_S or ψ_R is presented in fig. 9.

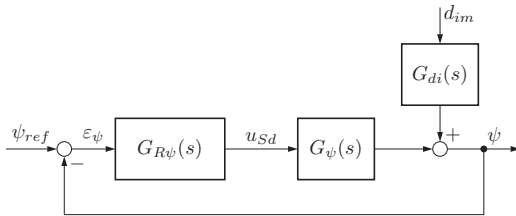


Fig. 9. Flux control system

The torque current i_{Sq} influences magnetising current i_{mR} in RFOC system which is presented in fig. 10, where PI controller approaches zero of the control error.

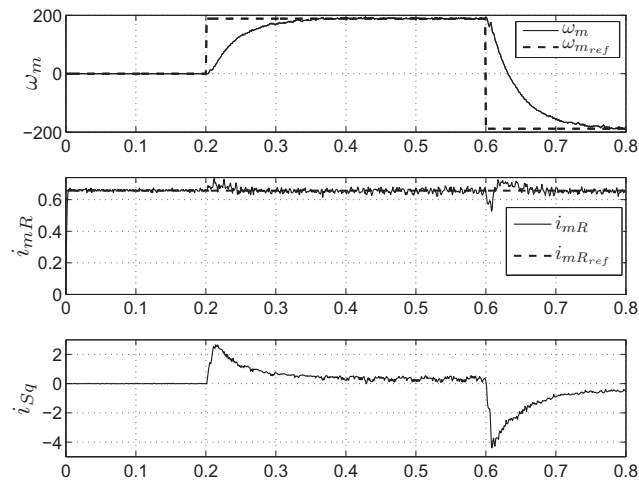


Fig. 10. Current i_{Sq} influence i_{mR} in RFOC

From relationship $\sigma T_R T_S < T_R + T_S$ models G_ψ can be approximated to first order lag element [27]. Thus, mathematical model of the motors with electromagnetic excitation is identical to (5e).

The rotor flux of permanent magnet motors is generated without any lag element (constant torque range – $i_{Sd} = 0$)

Electromagnetic torque circuit

Functional diagrams in fig. 2, 6 and 8 are similar to one another and one can derive closely to (5) formulas. Whereas,

SFOC and DTC-SVM methods (28) the additional disturbance are included $d_{\omega i}(s) = \mathcal{L}\{(p_b \omega_m - \omega_{mS})i_{Sd}\}$. From the transfer-function $G_{d2}(s)$ (s operator in numerator) it can be noticed that in steady-state signal $d_{\omega i}$ does not have any influence on the electromagnetic torque.

In the case of the model, which describes signal M_e , dynamics depends on the relation between constants B and T :

- $B \geq 4T$ second order lag element,
- $B < 4T$ oscillatory element.

Fig. 11 shows the influence of various values of the moment of inertia J (3kW squirrel-cage induction motor) to poles location of the transfer-function G_M .

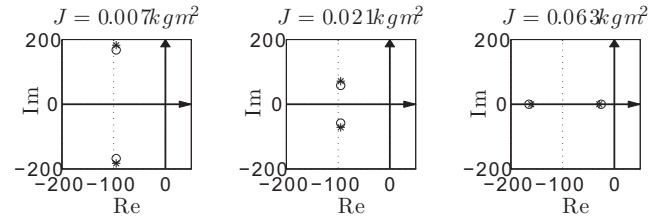


Fig. 11. Poles location of $G_M(s)$ – 'o' RFOC, '*' SFOC (DTC-SVM)

Differences between the eigenvalues of the systems can result from the errors of mathematical model for SFOC. Oscillations in the step responses of the systems decrease together with increasing J or decreasing value of the flux ψ_R or ψ_S (relation based on the electromechanical time constant formula B). This means that regardless the reference frame (ω^K) the mathematical model of the induction motor has similar eigenvalues.

The electromagnetic torque control system, which is based on the model (28) is shown in fig. 12. For remaining cases presented system does not include transfer-function $G_{d2}(s)$.

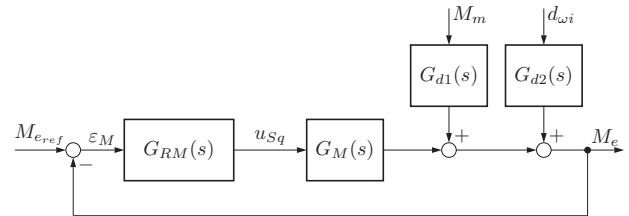


Fig. 12. Motor torque control system

From the locus of eigenvalues for any transfer-function $G_M(s)$ results that the standard simplification of the model to the lag element (neglecting the emf E) is not always proper. The results of such approximation and application of the modulus criterion are introduced in [28] and they show large divergences between real and desired responses.

Conclusion

The generalizations of the mathematical models of various motors and the reference frames were introduced in the article. In spite of the construction differences of respective electric motors, the mathematical models which were described determine the large similarity:

- The flux circuits are always non-oscillatory elements which one can reduce through approximation to the first order lag element.
- The voltage-electromagnetic torque relationship is the second order transfer-function and electromechanical T and electromechanical B time constants can be defined. On the basis of relationship among these constants one can specify if the motor is:

- $B \geq 4T$ second-order lag with derivative element,
- $B < 4T$ oscillatory with derivative element.
- *Field (flux) weakening*, that is the decreasing flux linkage (ψ_R, ψ_S or ψ_e) leads to electromechanical time constant B increases (5f), (19b) or (27b). Thanks to what, the damping of the system increases and the transfer-function $G_M(s)$ changes the location of poles.
- The dynamics of the induction motor does not depend on considered reference frame ($\omega^K = \omega_{mR}$ or $\omega^K = \omega_{mS}$).

The modulus criterion [1, 2] can be applied to parametric optimization of the PI flux controller. Whereas modulus criterion is also useful in optimization of the motor torque (one should predict the errors) or to apply the general-purpose, independent method of the model poles location [28, 29].

When controllers are designed one should test systems robustness on disturbance signals ($M_m, d_{im}, d_{\omega i}$) and here can be taken the advantage of robust control theory [22, 23].

It is advisable to check robustness of the control systems considering identification errors and parameters changes of mathematical models. One of the possibilities is applying the Kharitonov interval polynomials [30, 31].

BIBLIOGRAPHY

- [1] M. P. Kaźmierkowski and H. Tunia. *Automatic Control of Converter-Fed Drives*. Amsterdam, ELSEVIER, 1994.
- [2] M.P. Kaźmierkowski, R. Krishnan, and F. Blaabjerg. *Control in Power Electronics*. Academic Press, San Diego, 2002.
- [3] R. Krishnan. *Electric Motor Drives. Modelling, Analysis and Control*. NJ: Prentice Hall, 2001.
- [4] T. Orłowska Kowalska. *Bezczujnikowe układy napędowe z silnikami indukcyjnymi*. Oficyna Wydawnicza Politechniki Wrocławskiej, 2003.
- [5] W. Leonhard. *Control of Electrical Drives*. Berlin, Springer-Verlag, 1997.
- [6] G. Sieklucki. *Automatyka napędu*. Cracow, Wydawnictwa AGH, 2009.
- [7] P. Vas. *Sensorless Vector and Direct Torque Control*. Oxford University Press, 1998.
- [8] A.M. Trzynadłowski. *Control of Induction Motors*. Academic Press, San Diego, 2000.
- [9] R.D. Doncker, D.W.J. Pülle, and A. Veltman. *Advanced Electrical Drives: Analysis, Modeling, Control*. Springer, 2011.
- [10] D. W. Novotny and T. A. Lipo. *Vector Control and Dynamics of AC Drives*. Oxford University Press, 1996.
- [11] K. Bisztyga. *Sterowanie i regulacja silników elektrycznych*. Warszawa, WNT, 1989.
- [12] J Chiasson. *Modeling and High-Performance control of Electric Machines*. NJ: Wiley-IEEE Press, 2005.
- [13] B.K. Bose. *Modern Power Electronics and AC Drives*. NJ, Prentice Hall, 2002.
- [14] G.S. Buja and M.P. Kaźmierkowski. Direct torque control of PWM converter-fed ac motors—a survey. *IEEE Trans. Ind. Electron.*, 51(4):744–757, 2004.
- [15] X. Xue, X. Xu, T. G. Habetler, and Divan D. M. A low cost stator flux oriented voltage source variable speed drive. *Conf. Rec. IEEE-IAS Annu. Meeting*, 1:410–415, 1990.
- [16] C. Lascu, I. Boldea, and F. Blaabjerg. A modified direct torque control for induction motor sensorless drive. *IEEE Trans. Ind. Appl.*, 36(1):122–130, 2000.
- [17] C. Lascu and A. T. Trzynadłowski. A sensorless hybrid dtc drive for high-volume applications using the tms320f243 dsp controller. *Ind. Appl. Conference, 2001. Thirty-Sixth IAS Annual Meeting. Conference Record of the 2001 IEEE*, 1:482–489, 2001.
- [18] M. P. Kaźmierkowski, M. Żelechowski, and D. Świerczyński. Dtc-svm an efficient method for control both induction and pm synchronous motor. *In Proc. of the EPE-PEMC, 2004, Conf. 2-4 September, Riga, Latvia*, page on CD, 2004.
- [19] M. Żelechowski. *Space Vector Modulated-Direct Torque Controlled (DTC-SVM) Inverter-Fed Induction Motor Drive*. PhD thesis, Faculty of Electrical Engineering Institute of Control and Industrial Electronics, Warsaw University of Technology, 2005.
- [20] M. Zelechowski, M. Kaźmierkowski, and F. Blaabjerg. Controller design for direct torque controlled space vector modulated (dtsvm) induction motor drives. *IEEE ISIE, Dubrovnik, Croatia*, pages 951–956, 2005.
- [21] G. F. Blaabjerg, M. P. Kaźmierkowski, M. Zelechowski, D. Świerczyński, and W. Kołomyjski. Design and comparison direct torque control techniques for induction motors. *EPE'05, 11-14.09.2005, Dresden, Germany*, page on CD, 2004.
- [22] J.C. Doyle, B. Francis, and A. Tannenbaum. *Feedback Control Theory*. Macmillan Publishing, 1990.
- [23] S. Skogestad and I. Postlethwaite. *Multivariable feedback control: analysis and design*. John Wiley, 2005.
- [24] K. Zhou and J.C. Doyle. *Essentials of Robust Control*. NJ, Prentice Hall, 1998.
- [25] V. Utkin, J. Guldner, and J. Shi. *Sliding Mode Control in Electromechanical Systems*. London, Taylor & Francis, 1999.
- [26] G. Sieklucki, R. Sykuliski, and T. Orzechowski. Application of incremental encoder in direct field oriented control of permanent magnet synchronous motor. *Przeгляд Elektrotechniczny*, 86(3):216–220, 2010.
- [27] G. Sieklucki and T. Orzechowski. Model matematyczny napędu z silnikiem indukcyjnym – metoda dtc-svm. *Kraków, Elektrotechnika i Elektronika*, page in the press, 2010.
- [28] G. Sieklucki. Pole placement method for dc motor torque. *Archives of Control Sciences*, 19(3):307–324, 2009.
- [29] G. Sieklucki. Problem Iq regulatora momentu elektromagnetycznego. *Kraków, Elektrotechnika i Elektronika*, page in the press, 2010.
- [30] S. Białas. *Odporna stabilność wielomianów i macierzy*. Kraków, Uczelniane Wyd. Naukowo-Techniczne, 2002.
- [31] S.P. Bhattacharyya, H. Chapellat, and L.H. Keel. *Robust Control: The Parametric Approach*. NJ, Prentice Hall, 1995.

Authors: dr inż. Grzegorz Sieklucki

Akademia Górniczo-Hutnicza
Wydział Elektrotechniki, Automatyki, Informatyki i Elektroniki
Katedra Automatyki Napędu i Urządzeń Przemysłowych
al. Mickiewicza 30
30-059 Kraków
email: sieklo@kaniup.agh.edu.pl